



Photocatalytic activity of ZrO₂ nanoparticles prepared by electrical arc discharge method in water

Ali Akbar Ashkarran^{*}, Seyedeh Arezoo Ahmadi Afshar, Seyed Mahyad Aghigh, Mona kavianipour

Plasma Physics Research Center, Science and Research Branch, Islamic Azad University, P.O. Box 14665-678, Tehran, Iran

ARTICLE INFO

Article history:

Received 25 November 2009

Accepted 4 January 2010

Available online 11 January 2010

Keywords:

ZrO₂ nanoparticles

Arc discharge

Characterization methods

Photocatalytic activity

ABSTRACT

ZrO₂ nanoparticles were synthesized through arc discharge of zirconium electrodes in deionized (DI) water. X-ray diffraction (XRD) analysis of the as prepared nanoparticles indicates formation a mixture of nanocrystalline ZrO₂ monoclinic and tetragonal phase structures. Transmission electron microscopy (TEM) images illustrate spherical ZrO₂ nanoparticles with 7–30 nm diameter range, which were formed during the discharge process with 10 A arc current. The average particle size was found to increase with the increasing arc current. X-ray photoelectron spectroscopy (XPS) analysis confirms formation of ZrO₂ at the surface of the nanoparticles. Surface area of the sample prepared at 10 A arc current, measured by BET analysis, was 44 m²/g. Photodegradation of Rhodamine B (Rh. B) shows that the prepared samples at lower currents have a higher photocatalytic activity due to larger surface area and smaller particle size.

© 2010 Elsevier Ltd. All rights reserved.

1. Introduction

ZrO₂ nanoparticles have attracted much interest due to their specific optical and electrical properties and potential applications in transparent and optical devices, sensors, fuel cells, advanced ceramics and photocatalysts [1–4]. Specifically, much attention has been drawn towards their photocatalytic properties because of its application in environmental purification and decomposition of toxic and organic compounds. A key requirement for improving the photocatalytic activity is to increase the specific surface area and enhance the crystallinity [5]. These requirements are met by crystalline nanostructured materials. Several methods including hydrothermal [6], sol–gel [7], chemical vapor deposition (CVD) [8] and sputtering [9] have been used to prepare ZrO₂ nanoparticles. For efficient photocatalytic activity, nanomaterials need to be crystalline, that is, should be grown at high temperatures or at very slow rates. In general, synthesis of ZrO₂ usually results in amorphous structures but, electrical arc discharge in water has the advantage in this regard as it produces self-crystallized nanoparticles due to high temperature caused by joule heating. Moreover, compared with other techniques, electrical arc discharge in water is an attractive method because of simplicity of experimental set up, lack of need for complicated equipments, low impurity, less production steps leading to a high-throughput and cost-effective procedure to generate a high yield of nanoparticles. Also the simplicity of this method allows scaling up for mass production.

The early works by arc discharge method in liquids were based on production of carbonaceous nanostructures such as MWCNTs [10–13], SWCNTs, SW-CNHs [11] and nano-onions [13]. In past few years, few papers have been published regarding synthesis of metal and metal oxide nanostructures such as MoS₂ [14], CuO and Cu₂O [15], Ag [16,17], Au [18,19], WO₃ [20] and ZnO [21] by arc discharge in liquids.

In the present study, we report a simple, inexpensive and one-step synthesis route of ZrO₂ nanoparticles by arc discharge method in DI water. We have studied the effect of arc current on size distribution and the photocatalytic activity of the produced nanoparticles. The main advantage of the present method is the direct formation of ZrO₂ nanoparticles from discharge of zirconium electrodes within water. To the author's knowledge, to date there has been no published report on synthesis of ZrO₂ nanoparticles based on arc discharge using zirconium electrodes in DI water.

2. Experimental

2.1. Synthesis of ZrO₂ nanoparticles

The experimental set up consists of two main parts: a high current DC power supply and a reactor including anode, cathode and a micrometer which moves the anode towards the cathode. In this work, a 10–20 A current was applied between two zirconium metallic electrodes. The voltage was dropped to about 2–3.5 V during the arc formation while the current was fixed to a desired amount. Both the anode and cathode were wire shaped, 1 mm in diameter and had 99.2% purity (from Goodfellow). Initially, we bring the two electrodes into touch leading to a small contact cross

^{*} Corresponding author. Tel.: +98 21 44869632; fax: +98 21 44869640.
E-mail address: ashkarran@srbiu.ac.ir (A.A. Ashkarran).

section and thus to a high current density. Then we separate them from each other and as a result zirconium is ablated from the an-

ode and then condensed in water and forms different nanoparticles.

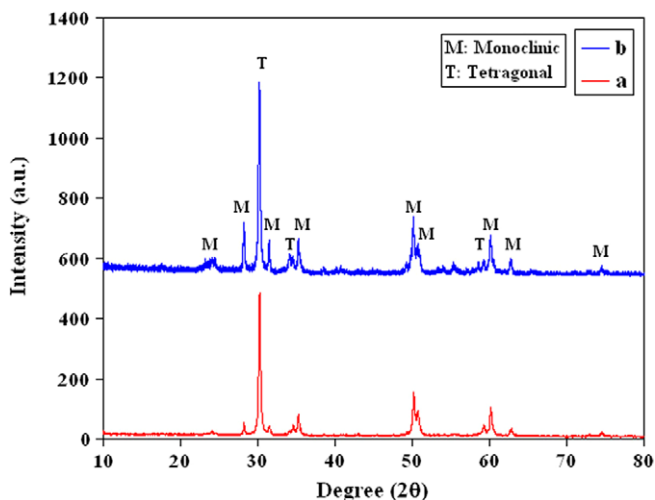


Fig. 1. XRD pattern of ZrO_2 nanoparticles was made at 10 A arc current (a) as prepared and (b) annealed at 500 °C.

2.2. Characterization

Analysis of the crystalline structures was performed by XRD diffractometer (X'pert Philips) with wavelength of $\text{Cu K}\alpha$ radiation in 2θ range from 10° to 80° by $0.005^\circ \text{ s}^{-1}$ steps. UV-Vis spectroscopy of the samples was taken out by a Lambda 950 spectrophotometer (Perkin-Elmer) from 200 nm to 1100 nm wavelengths. TEM analysis was performed by a LEO 912 AB instrument at 200 keV accelerating energy by deposition of ZrO_2 nanoparticles onto the copper grid at room temperature. XPS analysis was taken out by a dual Mg-Al anode X-ray source. A concentric hemispherical analyzer (from Specs company model EA10 plus) was employed to analyze the emitted electrons from the surface. The energy axis was calibrated by adjusting the carbon peaks at 285 eV. Surface area of the nanoparticles was determined by Belsorp adsorption-desorption (BEL Japan Inc.) instrument. Photocatalytic activity of the nanoparticles was measured by photodegradation of Rh. B with the initial concentration and volume of 10^{-5} M and 30 mL respectively at the presence of 30 mL ZrO_2 solution. First the mixed Rh. B and ZrO_2 solution was stirred in dark for 30 min to equilibrate the

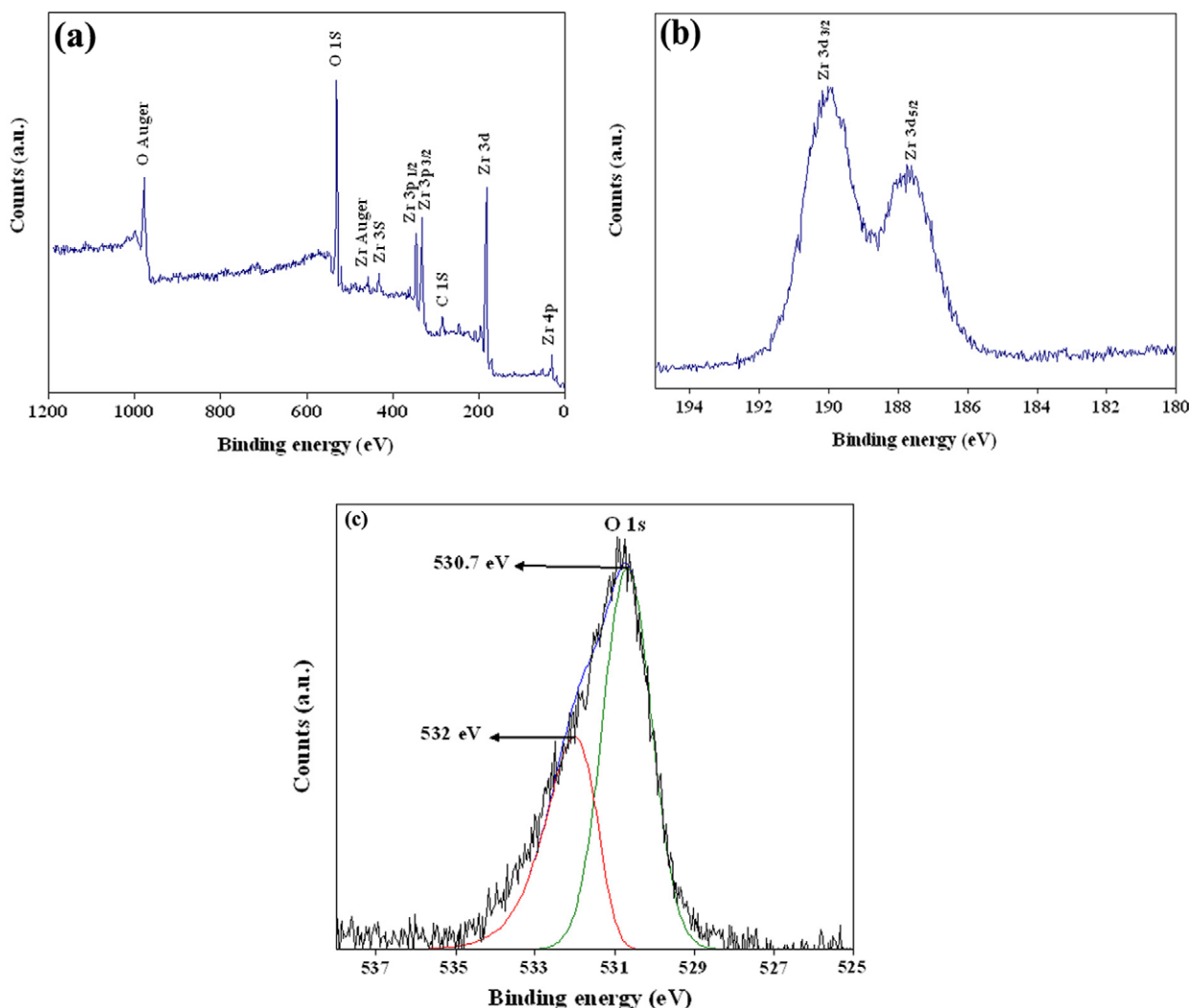


Fig. 2. XPS analysis for ZrO_2 nanoparticles formed at 10 A arc current, (a) wide range of energy survey, (b) energy range related to Zr peaks and (c) energy range related to O 1s peak.

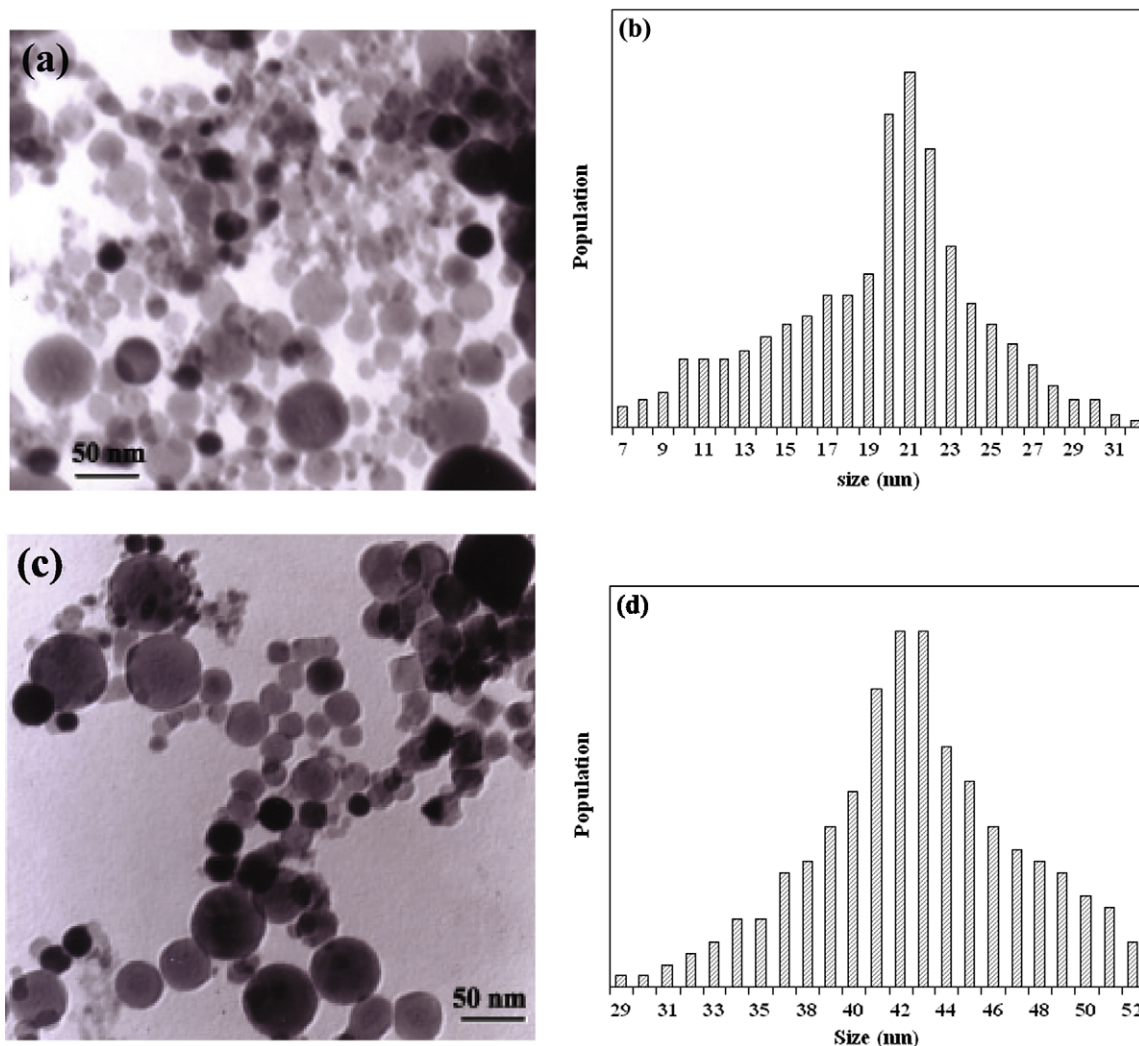


Fig. 3. TEM images of ZrO_2 nanoparticles prepared at (a) 10 and (b) 20 A electrical arc currents.

absorption–desorption between dye molecules and ZrO_2 photocatalysts. Then it was irradiated at room temperature by a 125 W low-pressure mercury lamp with 254 nm strongest peak wavelength. The degradation rate was measured by UV–Vis spectrophotometer at the maximum absorption wavelength of Rh. B. DI water was supplied from a Millipore water purification system (Direct-Q-3) with 18.2 M Ω cm (0.055 μ s) resistance.

3. Results and discussion

3.1. XRD analysis of the products

XRD result for as prepared samples at 10 A arc current demonstrates formation of crystalline ZrO_2 with a mixture of monoclinic and tetragonal phase which is depicted in Fig. 1. The obtained spectrum has the ZrO_2 monoclinic phase peaks at $2\theta = 24.5, 28.2, 31.5, 35.3, 50.2, 50.7, 60.1, 62.8, 72.9, 73.5$ and 74.6° and tetragonal phase peaks at $2\theta = 30.2, 34.6$ and 59.3° which is in agreement with the 37–1484 and 42–1164 standard card from the JCPDS. The single crystalline size determined by Debye–Scherrer formula was 16.5 nm. In this method the as prepared particles are usually crystallized due to high temperatures caused by joule heating. Annealing the extracted powder at 500 $^\circ$ C in air for 1 h did not result in any remarkable changes in the intensity or position of the peaks as is illustrated in Fig. 1b. The single crystalline size after heat

treatment was 17.5 nm which was approximately constant compared with before annealing. These results correspond to other works such as Zhang et. al. [22] and Liang et. al. [23].

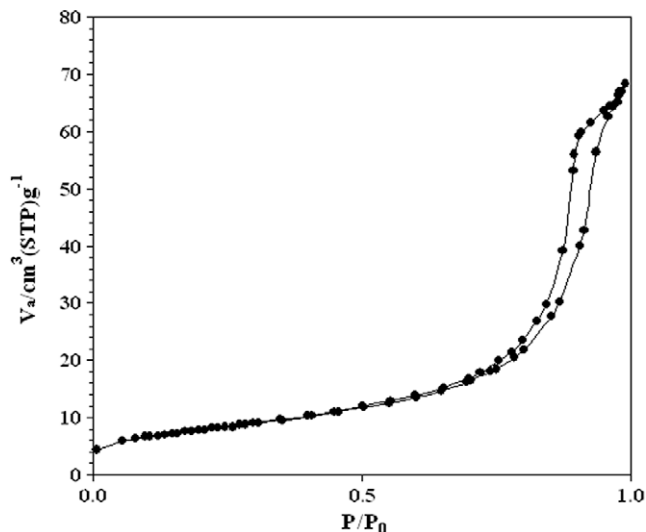


Fig. 4. BET adsorption–desorption analysis of as prepared ZrO_2 nanoparticles at 10 A arc current.

3.2. XPS analysis

To be sure about the composition of the product we performed XPS analysis. Fig. 2(a–c) shows the XPS data for the as-synthesized 10 A sample. From XPS spectrum the binding energies of O 1s, Zr 4p, Zr 3d, Zr 3p_{3/2}, Zr 3p_{1/2} and Zr 3s for the as prepared ZrO₂ nanoparticles are 530.7, 28.5, 181.5, 333, 346.5 and 433.5 eV, respectively. In addition a weak C 1s peak at 285 eV is observed due to ambient air contamination. To determine the chemical state we used Auger parameter of Zr (using Zr 3p_{3/2} peak and Auger peak at 459 eV) which is equal to 2011.2 eV. This value confirms formation of ZrO₂ at the surface of samples. Also O 1s peak (Fig. 2c) has two parts: main part at 530.7 which reflects ZrO₂ state and another part at 532 eV which is due to C–O bound. The ratio of oxygen to zirconium peaks determines O to Zr ratio about 2.2. The excess ratio from 2 is due to adsorbed oxygen at the surface of the sample.

3.3. TEM studies

The shape and size distribution of nanoparticles were characterized by TEM. Fig. 3 illustrates typical morphologies of ZrO₂ nanoparticles obtained at 10 and 20 A arc currents. It was observed

that the particles are nanosized and spherical. This means that the aspect ratio is close to 1. The histogram of the size distribution is shown in Fig. 3b. It imparts that the size of the particles is between 7 and 30 nm and the average diameter is 21 nm. TEM image and the related size distribution of the ZrO₂ nanoparticles synthesized at 20 A arc current is shown in Fig. 3c and d. It reveals that the size of the particles is between 30 and 52 nm and the average diameter is 42 nm. We can conclude that the mean particle size increases by increasing the arc current. The reason for this behavior has been discussed in detail in our previous work [19].

3.4. BET analysis

Photocatalytic activity of ZrO₂ nanoparticles depends on their surface area. In order to evaluate its activity we first determined the active surface area of the nanoparticles. BET analysis gives the surface area of the nanoparticles about 44 m²/g which is shown in Fig. 4. The adsorption–desorption isotherm shows a hysteresis loop that is very similar to type V isotherm [24]. The relationship between the specific surface area and the particle size in BET model is

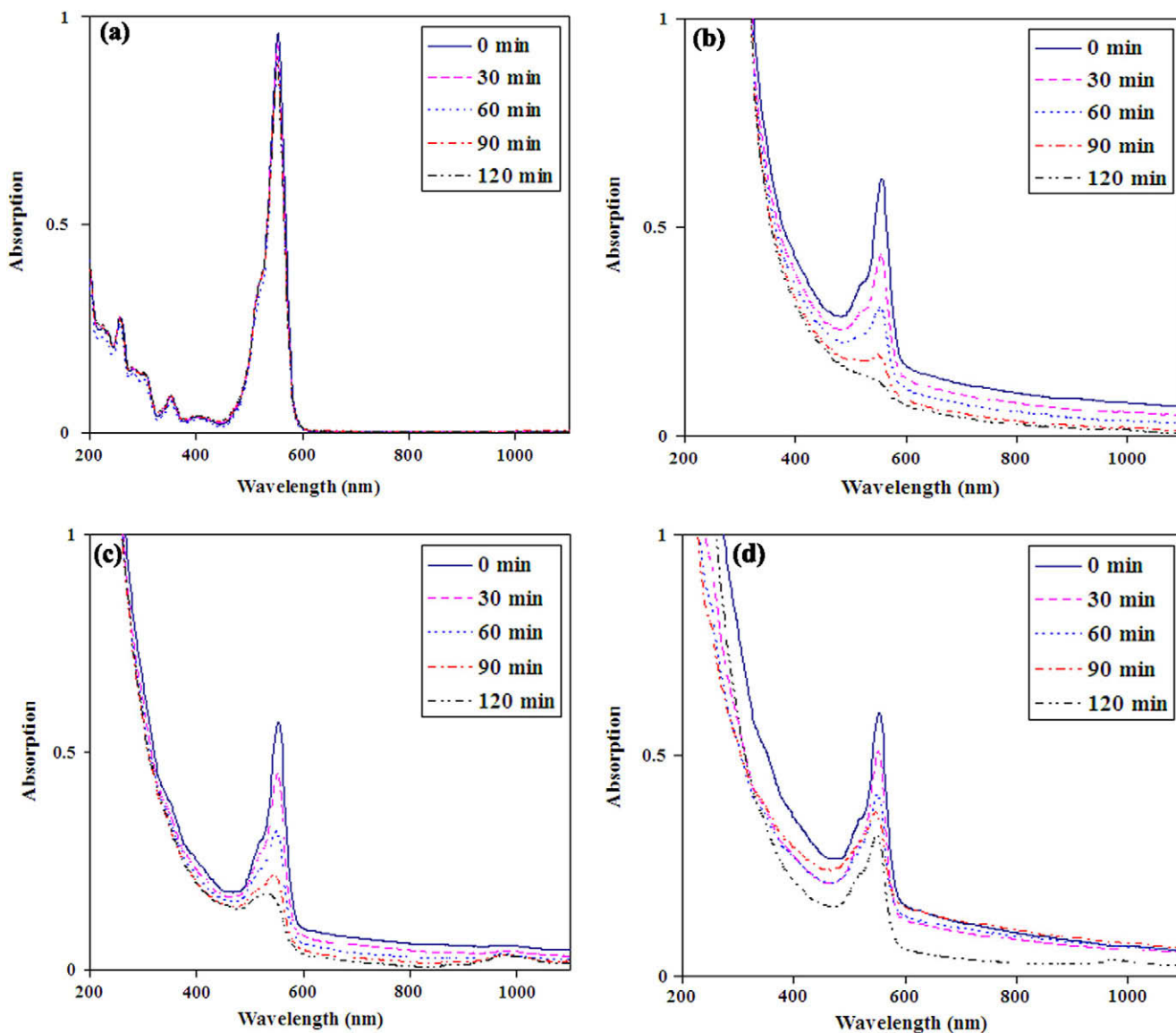


Fig. 5. Evaluating of photocatalytic activity of ZrO₂ nanoparticles by photodegradation of Rh. B. (a) Rh. B without ZrO₂ nanoparticles, (b) 10 A, (c) 15 A and (d) 20 A arc current.

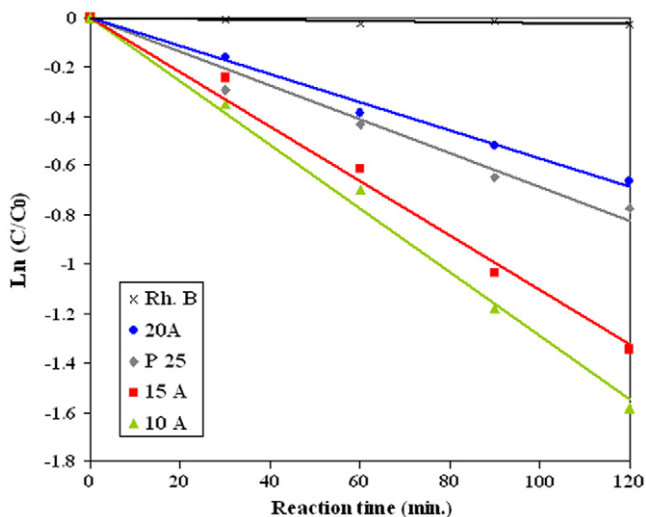


Fig. 6. Changes of rhodamine B concentration under UV illumination for the samples prepared at 10, 15 and 20 A arc currents and the blank sample.

$$S = \frac{6}{\rho d}$$

which ρ is the solid density, S is the specific surface area and d is the particle size. The average size of the nanoparticles calculated by this model is 24 nm which is in close agreement with TEM results.

3.5. Photocatalytic activity measurements

Changes in the absorption spectrum of Rh. B under UV illumination at different irradiation times for the samples made with 10, 15 and 20 A arc currents and one Rh. B sample as reference are illustrated in Fig. 5. No remarkable changes in the concentration of the Rh. B solution were observed in the absence of ZrO₂ nanoparticles (Fig. 5a). Therefore, decomposition of Rhodamine B only depends on the photoexcitation of ZrO₂ nanoparticles. The concentration and volume of all ZrO₂ samples were chosen at 10 mM and 30 mL, respectively, with 1:1 ratio of ZrO₂ to Rh. B for all measurements. We have measured yield and average production rate of ZrO₂ nanoparticles by measuring weight loss of the electrodes and duration of the arc process. To achieve same ZrO₂ concentration in all samples we have chosen 5, 3 and 2 s arc durations for 10, 15 and 20 A, respectively. It was observed that by increasing the irradiation time the maximum absorption peak decreases. This indicates that the concentration of Rh. B is decreasing at the presence of ZrO₂ nanoparticles and UV illumination, Fig. 5(b–d). Though all kinetic curves behave similarly, for the case of the larger particles photodegradation rate is less, as illustrated in Fig. 6. This can be due to higher surface area in samples with smaller size.

Photocatalytic reactions on ZrO₂ surface can be expressed by the Langmuir–Hinshelwood model [25]. The reaction rate after the adsorption equilibrium can be expressed as

$$-\ln(C/C_0) = Kt$$

where C and C_0 are the reactant concentration at time $t = t$ and $t = 0$, respectively, K and t are the apparent reaction rate constant and time, respectively. A plot of $-\ln(C/C_0)$ versus t will yield a slope

of K . The calculated reaction rate constant for the samples prepared at 10, 15 and 20 A arc currents were 16×10^{-3} , 14×10^{-3} and $5 \times 10^{-3} \text{ min}^{-1}$, respectively. Furthermore, compared with commercial TiO₂ photocatalyst (Degussa P25) in an equal situation, our 10 A sample shows near two times more photocatalytic activity.

4. Conclusion

We have prepared ZrO₂ nanoparticles in a one-step synthesis process by a high current electrical arc discharge of Zr electrodes in DI water. XRD results indicated formation of a mixture of nanocrystalline ZrO₂ monoclinic and tetragonal phase and 26.5 nm single crystalline domain size. Surface chemical composition of the nanoparticles determined by XPS shows formation of ZrO₂. TEM images revealed spherical nanoparticles with 21 and 42 nm mean particle size at 10 and 20 A arc currents, respectively. The particle size was found to increase with an increase in the arc current. Surface area of the sample prepared at 10 A arc current, measured by BET analysis, was 44 m²/g. Further, the photocatalytic activity of ZrO₂ nanoparticles demonstrated that by increasing UV illumination time, the maximum absorption peak and concentration of Rh. B decreases in the presence of ZrO₂ nanoparticles. In fact, decrease of concentration of the sample prepared at 10 A was found to be more pronounced than the sample prepared at 15 and 20 A arc current which was due to increased surface to volume ratio.

References

- [1] B. Zhu, C.R. Xia, X.G. Luo, *Thin Solid Films* 385 (2001) 209.
- [2] N.G. Petrik, D.P. Taylor, T.M. Orlando, *J. Appl. Phys.* 85 (1999) 6770.
- [3] A. Bastianini, G.A. Battiston, R. Gerbasi, M. Porchia, S. Daolio, *J. Phys.* 4 (1995) 525.
- [4] A. Corma, *Chem. Rev.* 95 (1995) 559.
- [5] G. Tian, K. Pan, H. Fu, L. Jing, W. Zhou, *J. Hazard. Mater.* 166 (2009) 939.
- [6] M.N. Tahir, L. Gorgishvili, J. Li, T. Gorelik, U. Kolb, L. Nasdala, W. Tremel, *Solid State Sci.* 9 (2007) 1105.
- [7] G. Ehrhart, B. Capoen, O. Robbe, P. Boy, S. Turrell, M. Bouazaoui, *Thin Solid Films* 496 (2006) 227.
- [8] A.M. Torres-Huerta, M.A. Dominguez-Crespo, E. Ramirez-Meneses, J.R. Vargas-Garcia, *Appl. Surf. Sci.* 255 (2009) 4792.
- [9] C. Roza, D. Jaque, L.F. Fonseca, J.G. Sole, *J. Lumin.* 128 (2008) 1197.
- [10] H. Lange, M. Sioda, A. Huczko, Y.Q. Zhu, H.W. Kroto, D.R.M. Walton, *Carbon* 41 (2003) 1617.
- [11] N. Sano, J. Nakano, T. Kanki, *Carbon* 42 (2004) 667.
- [12] N. Sano, H. Wang, I. Alexandrou, M. Chhowalla, K.B.K. Teo, G.A.J. Amaratunga, *J. Appl. Phys.* 92 (2002) 2783.
- [13] N. Sano, H. Wang, M. Chhowalla, I. Alexandrou, G.A.J. Amaratunga, *Nature* 414 (2001) 506.
- [14] I. Alexandrou, N. Sano, A. Burrows, R.R. Meyer, H. Wang, A. Kirkland, C.J. Kiely, G.A.J. Amaratunga, *Nanotechnology* 14 (2003) 913.
- [15] W.T. Yao, S.H. Yu, Y. Zhou, J. Jiang, Q.S. Wu, L. Zhang, J. Jiang, *J. Phys. Chem. B* 109 (2005) 14011.
- [16] C.H. Loa, T.T. Tsung, H.M. Lin, *J. Alloys Compd.* 434–435 (2007) 659.
- [17] A. A. Ashkarran, A. Irajizad, M. M. Ahadian, M.R. Hormozi Nezhadi, *Eur. Phys. J. Appl. Phys.* 48 (2009) 10601.
- [18] J.K. Lung, J.C. Huang, D.C. Tien, C.Y. Liao, K.H. Tseng, T.T. Tsung, W.S. Kao, T.H. Tsai, C.S. Jwo, H.M. Lin, L. Stobinski, *J. Alloys Compd.* 434–435 (2007) 655.
- [19] A.A. Ashkarran, A. Irajizad, S.M. Mahdavi, M.M. Ahadian, M.R. Hormozi Nezhad, *Appl. Phys. A* 96 (2009) 423.
- [20] A.A. Ashkarran, A. Irajizad, M.M. Ahadian, S.A. Mahdavi Ardakani, *Nanotechnology* 19 (2008) 195709.
- [21] A.A. Ashkarran, A. Irajizad, S.M. Mahdavi, M.M. Ahadian, *Mater. Chem. Phys.* 118 (2009) 6.
- [22] Y.W. Zhang, X. Sun, G. Xu, C.H. Yan, *Solid State Sci.* 6 (2004) 523.
- [23] J. Liang, X. Jiang, G. Liu, Z. Deng, J. Zhuang, F. Li, Y. Li, *Mater. Res. Bull.* 38 (2003) 161.
- [24] S.J. Gregg, K.S.W. Sing, *Adsorption Surface Area and Porosity*, Academic Press, 1982.
- [25] D.L. Liao, C.A. Badour, B.Q. Liao, *J. Photochem. Photobiol. A* 194 (2008) 11.